Supporting Information

Sonochemical edge functionalisation of molybdenum disulphide

Aline Amorim Graf [†,*], Matthew J. Large[†], Sean P. Ogilvie[†], Yuanyang Rong[†], Peter J. Lynch[†], Giuseppe Fratta[†], Santanu Ray[‡], Aleksey Shmeliov[§], Valeria Nicolosi[§], Raul Arenal[⊥,ǁ,o], Alice A. K. King[†], and Alan B. Dalton[†,*]

[†] University of Sussex, Brighton, BN1 9QH, UK

[‡] Surface Analysis Laboratory, University of Brighton, Brighton, BN2 4GJ, UK

[§] Trinity College Dublin, School of Chemistry, CRANN, AMBER & I-Form, Dublin 2, Dublin, Ireland

[⊥] Laboratorio de Microscopias Avanzadas, Instituto de Nanociencia de Aragón, Universidad de Zaragoza, 50018 Zaragoza, Spain

[ǁ] ARAID Foundation, 50018 Zaragoza, Spain

[o] Instituto de Ciencias de Materiales de Aragon, CSIC-U. de Zaragoza, 50009 Zaragoza, Spain

Table of Contents

1. FWHM histogram of Raman mode

Non-resonant Raman mapping shows a broadening in full width at half maximum for MoS_2 exfoliated in acetone which is associated with a larger defect density[1].

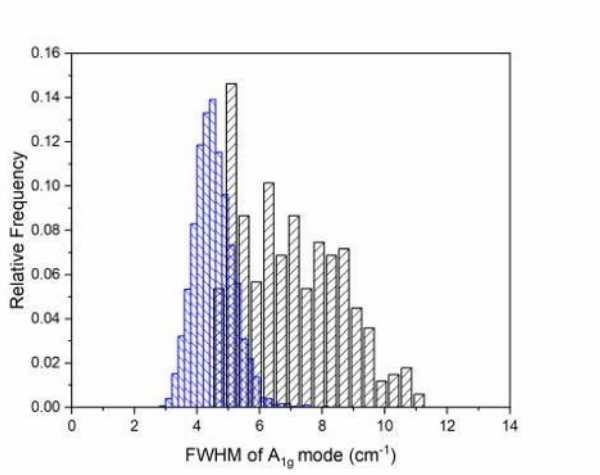

Figure S1: Histogram of FWHM of out-of plane (A_{1g}) mode for MoS_2 exfoliated in acetone (black) and IPA (blue).

2. Additional TEM micrographs

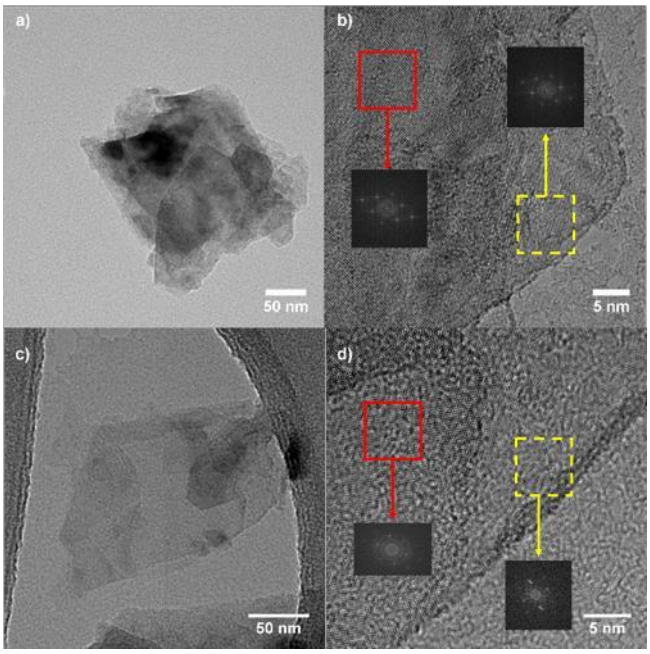

Figure S2. a) Representative TEM micrograph of MoS_2 exfoliated in isopropanol. b) Zoomed in TEM micrograph of the same dispersion with an inset showing the FFT as a regular hexagonal structure for both basal plane (red) and edges (yellow) of the flakes. c) Representative TEM micrograph of MoS_2 flake casted from the dispersion in acetone. d) Edge of an acetone-exfoliated MoS_2 flake. Inset shows the expected hexagonal pattern for the basal plane (red) and a different pattern at the edges (yellow) corresponding to few-layered molybdenum trioxide.

3. XPS data for acetone-exfoliated nanosheets in the range of sulfur energy

XPS characterisation showing the range for sulfur binding energy confirming that MoS_2 is the only sulfur-containing compound in the sample.

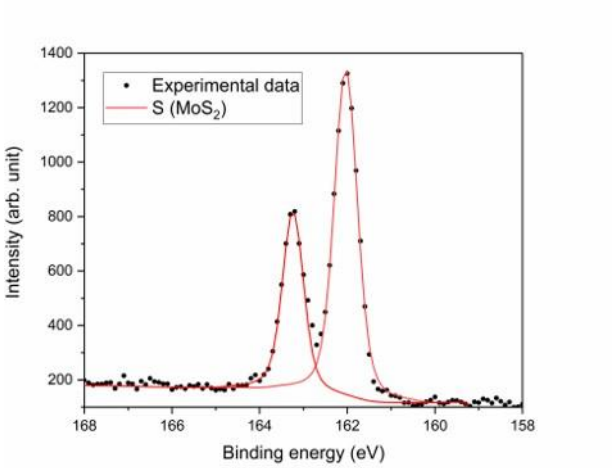

Figure S3: XPS spectrum in the range of sulfur binding energy for acetone-exfoliated nanosheets.

4. Zeta potential characterisation

Zeta potential measurements for the sonication time study are shown in Figure S4. Stable dispersions are produced even at short sonication times.

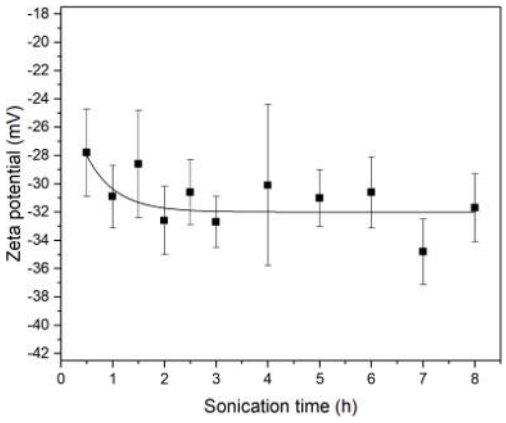

Figure S4. Zeta potential measurements for sonication time study.

5. Hansen and Hildebrand parameters measurement

Hansen and Hildebrand solubility parameters were measured for a dispersion (supernatant) and unexfoliated bulk crystallites (sediment of the final centrifugation step after the sonication). Figure S5 shows Hildebrand parameters for the unexfoliated flakes. Hansen parameters for both materials are shown in Figure S6. Comparing the results with accepted values, as seen in Table 1, show a significant change in the polar

component between these two fractions. Hansen solubility parameters for MoO_3 were estimated by analysing data in literature[2].

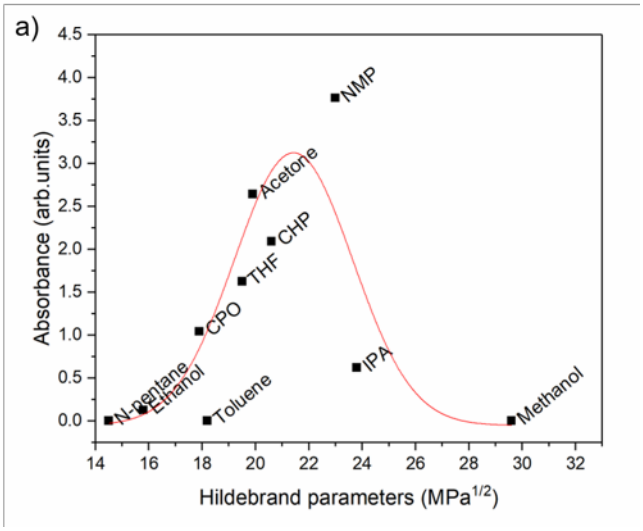

Figure S5. Hildebrand solubility parameters for unexfoliated MoS_2 flakes.

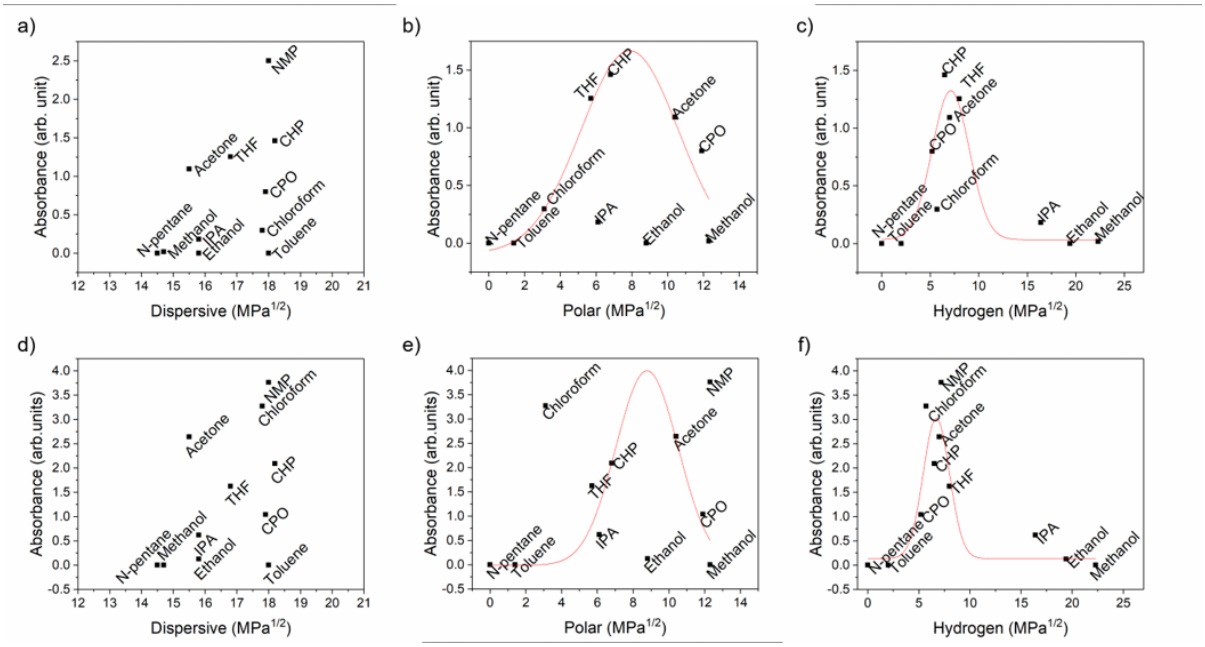

Figure S6. Hansen solubility parameters for a-c) dispersion and d-f) unexfoliated crystallites.

Table 1. Hansen and Hildebrand parameters for exfoliated MoS_2 and bulk powder.

	Dispersive Hansen parameter ($MPa^{1/2}$)	Polar Hansen parameter ($MPa^{1/2}$)	Hydrogen Hansen parameter ($MPa^{1/2}$)	Hildebrand parameter ($MPa^{1/2}$)
MoS_2[3]	18	8.5	7.0	21.1
MoO_3[2]	18	7.1	6.4	20.7
MoS_2/ acetone (dispersion)	17.91	7.87±0.36	7.10±0.38	20.81±0.63

MoS_2/ acetone (sediment)	18.37	8.77±0.23	6.70±0.29	21.43±0.55
Acetone[4]	15.5	10.4	7.0	19.9

6. Raman map for MoS_2 nanosheets exfoliated in 2-butanone

A dispersion of MoS_2 in 2-butanone (purchased from Sigma Aldrich) was prepared following the same exfoliation procedure described for acetone. A non-resonant Raman map using the same parameters for acetone-exfoliated sample is shown in figure S7a with a representative spectrum taken from the map. Figure S7b is a plot of the second derivative of Raman spectra for two different solvents: acetone (black) and 2-butanone (red). The second derivative clearly shows the position of local minima and maxima points, which can be correlated to Raman modes positions. The oxide modes identified in Figure 3 are highlighted.

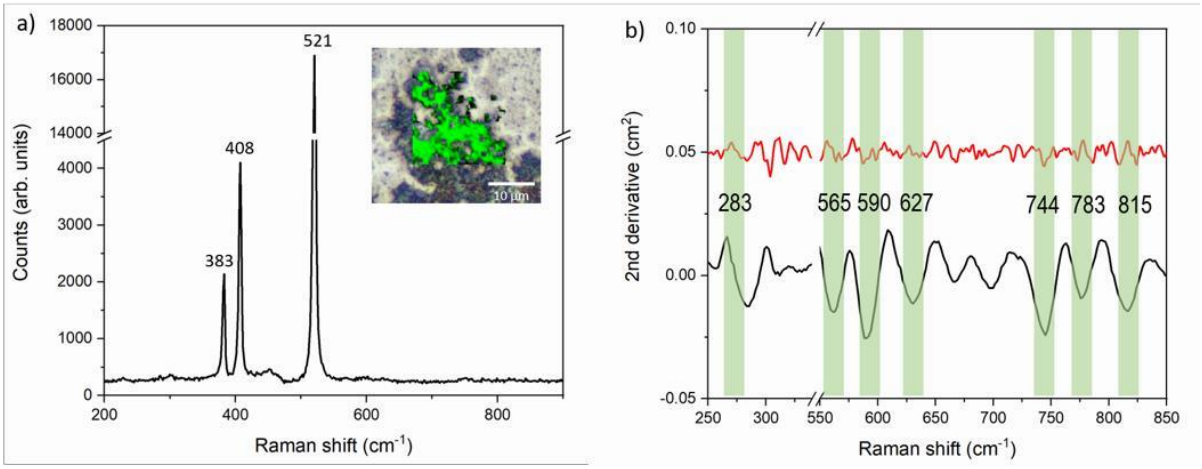

Figure S7: a) Representative Raman spectrum from a dispersion of MoS_2 exfoliated in 2-butanone map (inset). b) Second derivative plot of Raman spectra for MoS_2 exfoliated in acetone (black) and 2-butanone (red) in the range of observed oxide modes. Highlighted areas are correlated to peak assignment done in Figure 3.

References

1S. Mignuzzi, A. J. Pollard, N. Bonini, B. Brennan, I. S. Gilmore, M. A. Pimenta, D. Richards and D. Roy, *Phys. Rev. B*, 2015, **91**, 1954111–7.

2D. Hanlon, C. Backes, T. M. Higgins, M. Hughes, A. O'Neill, P. King, N. McEvoy, G. S. Duesberg, B. Mendoza Sanchez, H. Pettersson, V. Nicolosi and J. N. Coleman, *Chem. Mater.*, 2014, **26**, 1751–1763.

3G. Cunningham, M. Lotya, C. S. Cucinotta, S. Sanvito, S. D. Bergin, R. Menzel, M. S. P. Shaffer and J. N. Coleman, *ACS Nano*, 2012, **6**, 3468–3480.

4C. M. Hansen, *Hansen solubility parameters: a user's handbook*, CRC Press, Boca Raton, 2nd ed., 2007.